

# Dislocation Processes and Deformation Twinning in Nanocrystalline Al

V. Yamakov\*, D. Wolf\*, S. R. Phillpot\*, and H. Gleiter\*\*

\* Argonne National Laboratory, Argonne, IL 60439, USA

\*\* Forschungszentrum Karlsruhe, D-76021 Karlsruhe, Germany

## ABSTRACT

Using a recently developed, massively parallel molecular-dynamics (MD) code for the simulation of polycrystal plasticity, we analyze for the case of nanocrystalline Al the complex interplay among various dislocation and grain-boundary processes during low-temperature deformation. A unique aspect of this work, arising from our ability to deform to rather large plastic strains and to consider a rather large grain size, is the observation of deformation under very high grain-boundary and dislocation densities, i.e., in a deformation regime where they compete on an equal footing. We are thus able to identify the intra- and intergranular dislocation and grain-boundary processes responsible for the extensive deformation twinning observed in our simulations. This illustrates the ability of this type of simulations to capture novel atomic-level insights into the underlying deformation mechanisms not presently possible experimentally.

## 1 INTRODUCTION

The mechanical behavior of nanocrystalline materials (i.e., polycrystals with a grain size of less than 100 nm) remains controversial [1], the observations ranging from greatly enhanced ductility [2-4] to dramatically increased strength and hardness [5-7]. While it is commonly accepted that the intrinsic deformation behavior of these fascinating materials must arise from the dynamical interplay between dislocation and grain-boundary (GB) processes [8], little is known to date on the specific deformation mechanisms. Here we describe large-scale molecular-dynamics (MD) simulations of nanocrystalline-Al model microstructures which begin to elucidate this intricate, highly non-linear interplay during room-temperature plastic deformation. We hope to demonstrate that these simulations have now advanced to a level where they provide a powerful new tool not only for exposing the atomic-level mechanisms controlling the complex dislocation-dislocation interaction processes in heavily deformed nanocrystals, but also for elucidating the response of the GB network to internal and external stresses.

The common low-temperature plastic-deformation mechanism in most metals and ceramics involves the continuous nucleation of dislocations from Frank-Read sources and their glide, on well-defined slip systems, through the crystal. In a polycrystalline material the size of these sources cannot exceed the grain size. Since the stress needed for their operation is inversely proportional to the

size of the source, this deformation mechanism can operate only down to a grain size of typically about 1  $\mu\text{m}$ . For a smaller grain size, mobile dislocations must be nucleated from other sources, such as the GBs or grain junctions.

## 2 SIMULATION APPROACH

To address this question, recent MD simulations of rather simple,  $\langle 110 \rangle$  textured Al polycrystals with a grain size of up to 70 nm revealed the onset of plastic flow when the applied tensile stress exceeds the threshold stress for the nucleation of dislocations from the GBs or grain junctions. [9] Idealized microstructures consisting of four grains of identical size and a regular-hexagonal shape were considered (see Fig. 1); the grain orientations were chosen such that all 12 GBs in the simulation cell are asymmetric high-angle  $\langle 110 \rangle$  tilt boundaries. The  $\langle 110 \rangle$  column axis was chosen such that, following their nucleation, dislocations can glide in each grain on either of two (111) slip systems, unimpeded by the three-dimensionally periodic border conditions imposed on the simulation cell.

A many-body interatomic potential for Al fitted, among other parameters, to the elastic constants is used [10] The potential has been slightly modified for a higher degree of smoothness at the cut-off radius [9]. While leaving other physical parameters practically unchanged, this modification increases the stacking-fault energy from 104 [10] to 122  $\text{mJ/m}^2$  [9], i.e., closer to the experimental values [11] ranging between 120 and 142  $\text{mJ/m}^2$ .

## 3 SIMULATION RESULTS

Figure 1 illustrates the emission of an *extended*  $1/2[011]$  dislocation into grain 2 from a GB in the vicinity of a triple junction. [9] The complete nucleation process involves the successive emission of both the leading and trailing Shockley partials (seen as the terminating black atoms) connected by a stacking fault (light-gray atoms). Following their complete nucleation, these extended dislocations travel across the grains on one of the available (111) slip planes, until they annihilate in the opposite GB, converting their Burgers vector into plastic strain.

It is interesting to note that for low plastic strain (i.e., in the absence of dislocation-dislocation interactions), the deformation is essentially reversible: on unloading the sample, the dislocation disappears by gliding back to the GB sites from which it nucleated, to be re-incorporated into the GB structure. (A movie demonstrating this process is posted at [www.msdl.anl.gov/im/movies/deform.html](http://www.msdl.anl.gov/im/movies/deform.html).) As the grain

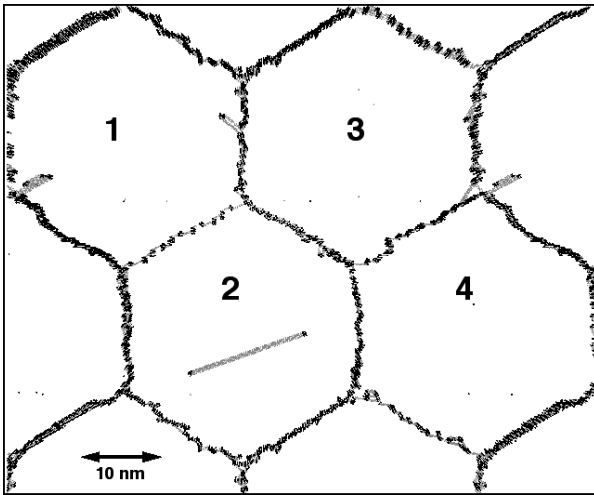
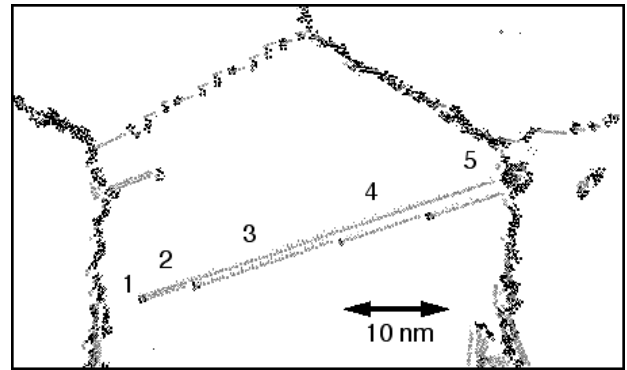


Figure 1. Snapshot of a  $\langle 110 \rangle$  textured Al polycrystal with a grain size of 30 nm after 27.6 ps of tensile deformation under a stress of 2.3 GPa applied in the horizontal direction at 300 K. A complete, extended dislocation emitted from the GB on the left is traveling across grain 2. Common-neighbor analysis [12] was used to identify perfect-crystal atoms as being either in a local hcp (light-gray atoms) or fcc environment (atoms not shown). Black atoms are ‘defected atoms’, i.e., atoms neither in an fcc nor hcp environment.

size decreases down to about 20 nm, nucleation of complete dislocations is no longer possible and the dislocation-slip mechanism seizes to be operational [9], in favor of a GB-based deformation mechanism. [13,14]

Deformation twinning represents another powerful elementary deformation process associated with the nucleation of partial dislocations from the GBs. In agreement with the well-known mechanism described in the literature [15], the mechanism observed in our simulations (see Fig. 2, [16]) reveals that the process occurs by the successive emission of partial dislocations onto adjacent (111) planes from the same GB. The stacking sequences of the three types of (111) planes, labeled A, B and C, in five regions of the twinned grain are indicated in the bottom of the figure. These regions are: 1. perfect fcc crystal; 2. intrinsic stacking fault; 3. extrinsic stacking fault; 4. two twin boundaries separated by two (111) planes, and 5. further broadened twin.

As the plastic strain increases, the dislocation concentration in the grain interiors gradually increases, eventually giving rise to various types of dislocation-dislocation interaction processes associated with the glide of extended dislocations on different slip systems but in the same grain. Most of these processes are well-known from extensive deformation studies in single crystals and coarse-grained polycrystals. [17] Among the best known is the formation of Lomer-Cottrell locks, seen in each of the four grains in Fig. 3 below. These locks are formed at the intersection between two extended dislocations on different



1. ABCABCABCABCABCABC
2. ABCA|B|ABCABCABCABC
3. ABCA|B|A|C|ABCABCABC
4. ABCA|B|A|C|B|C|ABCABC
5. ABCA|B|A|C|B|C|B|C|ABC

Figure 2. Formation of a twin lamella (or ‘deformation twin’) by the successive emission of identical partial dislocations from the same GB onto neighboring slip planes; the grain diameter is 45 nm. As in Fig. 1, light-gray atoms indicate a perfect-crystal hcp environment, black atoms are ‘defected’ and gray atoms symbolize perfect-crystal fcc atoms. The stacking sequences of the three types of (111) planes, labeled A, B and C, in five regions of the twinned grain are indicated in the bottom of the figure.

slip planes, terminated by Shockley partials that attract each other.

In addition to the effects associated with the interactions between gliding dislocations, for larger strains our simulations reveal a variety of unanticipated and intriguing effects arising from the interaction of dislocations with GBs and with deformation twins. Their net combined effect after  $\sim 12\%$  plastic strain is shown in the snapshot in Fig. 3 for a grain size of 45 nm.

The considerable roughness of the initially flat GBs is particularly noticeable (compare with Fig. 1). Moreover, beyond a plastic strain of about 8%, a new grain (labeled A) is seen to nucleate at those GBs that had been particularly active during these emission/absorption events.

The roughness of the GB network arises in part from the continuous nucleation and annihilation of dislocations. In addition, Fig. 3 demonstrates a mechanism for what, at first sight, appears to be GB splitting (see the GB between grains 2 and 3). However, detailed analysis reveals that the ordered deformation substructure in grain 2 arises from the emission of a series of *extrinsic* stacking faults from the GB, by the nucleation of double-Shockley partials (compare with region (3) in Fig 2). Interestingly, these cores are aligned in a straight line, presumably due to elastic interactions among them, and eventually leading to the formation of a new dislocation boundary.

This nucleation of double-Shockley partials represents another elementary deformation process associated with the

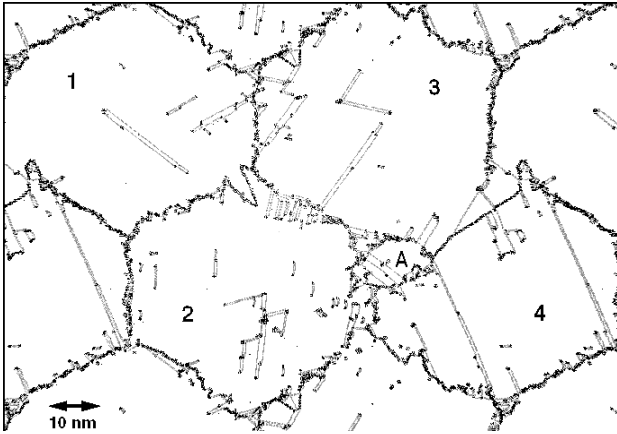


Figure 3. Snapshot at 11.9% plastic strain for a grain diameter of 45 nm. A variety of processes involving dislocation-dislocation and dislocation-GB interactions has taken place during the deformation. (A movie of the full deformation simulation is posted at [www.msd.anl.gov/im/movies/deform.html](http://www.msd.anl.gov/im/movies/deform.html).)

nucleation of dislocations from the GBs. It is known, however, that this process requires very large local stresses.

The most intriguing process in Fig. 3 involves the nucleation of the new grain, A. The sequence of snapshots in Fig. 4 captures in detail the underlying GB and dislocation processes. The nucleation of the new grain starts by the emission of a complete  $1/2[110]$  dislocation from the GB between grains 3 and 4 (process (1) in (a)). The complex core structure labeled (1') was formed by two such dislocations, emitted however onto different slip planes. As seen in (b), this new, virtually immobile complex core structure subsequently begins to continuously emit partials, producing a growing twin lamella by 'partial-dislocation breakaway' [17], process (2). This lamella grows further by absorbing additional  $1/2[110]$  dislocations emitted from the same GB (process (1) in (b)), leading to its increased size in (c). As also seen from (c), the development of the new grain also involves the emission of another twin lamella (labeled (3)) together with extrinsic stacking faults terminated by double-Shockley partials (labeled (4); see also process 7 in Fig. 1). Finally, the rather complex deformation substructure thus formed subsequently coalesces to form the final grain A in (d) and Fig. 3.

In coarse-grained Al, the propensity for deformation twinning observed in Figs. 1 - 4 would be very surprising, given that Al has a rather high stacking-fault energy. However, it is also known that the relationship between the stacking-fault energy and the occurrence of deformation twinning is rather indirect and, in fact, entirely unexplored in nanocrystalline materials. [18] Our observations strongly suggest that a reexamination of the basic models for twinning, with particular emphasis on nanocrystalline grain size, may be timely.

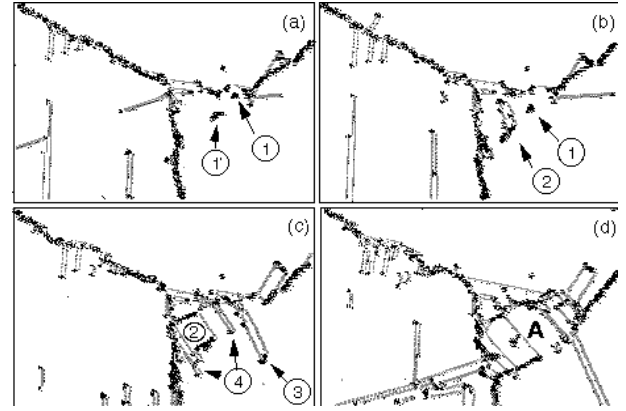


Figure 4. Successive snapshots of the vicinity of the triple junction connecting grains 2, 3 and 4, demonstrating the mechanism by which the new grain A in Fig. 2 was formed. (a)  $\epsilon=6.09\%$  plastic strain; (b) 6.19%; (c) 6.76% and (d) 8.71%. Four distinct processes labeled (1) – (4) are revealed; these are described in the text.

## 4 CONCLUSIONS

In large part, our simulations cover entirely new, experimentally as of yet unexplored ground, not only as far as the small grain size is concerned but also in other important aspects. By contrast with typical in-situ transmission-electron-microscopy experiments, the insights gained from Figs. 3 and 4 capture inherently bulk deformation behavior, unencumbered by any mechanical stresses and surface effects that inadvertently affect the observations in thin-film specimens. Also, even for coarse-grained materials it would be extremely difficult to extract from experiments, in the type of dynamical and atomistic detail available from Figs. 3 and 4, the underlying deformation mechanisms.

The above simulations of well-characterized, albeit highly idealized model systems illustrate the exciting new opportunities offered by large-scale MD simulations towards unraveling the complex interplay between the dislocation and GB processes in polycrystalline materials. However, it is equally important to be aware of the fundamental limitations inherent to this approach. Apart from being limited to relatively small systems, by their very nature MD simulations are restricted to very high stresses and strain rates, many orders of magnitude higher than experimental rates. For example, a strain of 1% occurring in 10 ns of simulation time corresponds to a strain rate of  $10^6 \text{ s}^{-1}$ .

Concerning the present simulations, in spite of the large tensile stresses (of 2.3 GPa) and strain rates ( $\sim 10^7 \text{ s}^{-1}$ ) under which deformation was observed, typical dislocation-glide velocities in our simulation (of about 500 m/s) are well below the sound velocity (of about 3664 m/s in the [100] direction obtained by simulation, compared to the experimental value of 3050 m/s). More importantly, however, the resolved shear stresses, of the order of 1 GPa on the (111) slip planes of our system, are well below the theoretical shear strength,  $\sigma_{th}$ , for Al. Frenkel's perfect-

crystal shear model gives an estimate of  $\sigma_{th}=G/2\pi$ ; with  $G=32.5$  GPa for Al at 0K (to which our potential was fitted<sup>10</sup>), we obtain a value of  $\sigma_{th}=5.18$  GPa at 0K, and slightly lower at room temperature. This value is in good agreement with recent nanoindentation experiments on Al thin films which yielded values of  $\sigma_{th}$  in the range of 4.2 – 4.5 GPa [19], leading the authors to conclude that the Frenkel formula is well satisfied for Al.

In summary, our simulations provide atomic-level insights into dislocation - GB interaction processes in nanocrystalline materials never before seen in either experiments or simulations, and with a degree of mechanistic detail not presently possible by experiments. They thus offer a glimpse of how, in the near future, such simulations may revolutionize our understanding of plastic deformation processes in heavily deformed materials. In particular, it should soon be possible to elucidate the physical mechanisms controlling technologically important processes, such as superplastic forming. Moreover, the ability of such simulations to completely characterize the highly inhomogeneous state of internal stress will undoubtedly spur the development of better materials-physics based deformation models.

### ACKNOWLEDGEMENTS

V.Y., D.W. and S.R.P. are supported by the US Department of Energy, BES-Materials Science under contract W-31-109-Eng-38. V.Y. is also grateful for support from the DOE/BES-MS Computational Materials Science Network (CMSN). We benefited from useful discussions with A. K. Mukherjee (University of California).

### REFERENCES

1. Koch, C.C. & Suryanarayana, C. in *Microstructure and Properties of Materials*, Vol. 2, , (Ed. J.C.M. Li, World Scientific Publishing, Singapore (2000)) 380-385.
2. Karch, J., Birringer, R., and Gleiter, H. *Nature* 330, 556, 1987.
3. McFadden, S.X., Mishra, R.S., Valiev, R.Z., Zhilyaev, A.P, and Mukherjee, A.K, *Nature* 398, 684, 1999.
4. Kim, B.N., Hiraga, K., Morita, K. and Sakka, Y., *Nature* 413, 288, 2001.
5. Siegel, R.W., *Mat. Sci.Forum* 235-238, 851, 1997.
6. Morris, D.G. & Morris, M.A., *Mat. Sci. Forum* 235-238, 861, 1997.
7. Nesladek, P. and Veprek, S. *Physica Status Solidi A* 177, 53, 2000.
8. See e.g., Yip, S., *Nature* 391, 532, 1998.
9. Yamakov, V., Wolf, D., Salazar, M., Phillpot S.R. and Gleiter, H. *Acta mater.* 49, 2713, 2001.
10. Ercolessi, F. & Adams J. B., *Europhys. Lett.* 26, 583, 1994.
11. Noonan, J.R. & Davis H.L. *Phys. Rev. B* 29, 4349, 1984.
12. Jonsson, H. and Andersen, H.C. *Phys. Rev. Lett.* 60, 2295, 1988.
13. Schiotz, J., DiTolla, F.D., Jacobsen, K.W., *Phys. Rev. B* 60, 11971, 1999.
14. Swygenhoven, H.V., Spaczer, M., Caro, A. and Farkas, D. *Phys. Rev. B* 60, 22, 1999.
15. Weertman, J., and Weertman, J.R. *Elementary dislocation theory.* (Oxford University Press, New York, Oxford, 1992).
16. Yamakov, V. and Salazar, M., unpublished work.
17. Hirth, J.P. and Lothe, J. *Theory of Dislocations.* (John Wiley & Sons, Inc., 1992).
18. El-Danaf, E., Kalindi, S.R., and Doherty, R., *Met. & Mat. Trans.* 30A, 1223, 1999.
19. Gouldstone, A, Koh, H.-J, Zeng, K.-Y, Giannakopoulos, A.E., & Suresh, S. *Acta mater.* 48, 2277, 2000.